INTERFACE

rsif.royalsocietypublishing.org

Research

Cite this article: Chen Z, Guo Q, Dai E, Forsch N, Taber LA. 2016 How the embryonic chick brain twists. *J. R. Soc. Interface* 20160395. http://dx.doi.org/10.1098/rsif.2016.0395

Received: 19 May 2016
Accepted: 20 October 2016

Subject Category:
Life Sciences–Engineering interface

Subject Areas:
biomechanics, biophysics, bioengineering

Keywords:
left–right asymmetry, embryonic development, torsion, biomechanics, axial rotation

Author for correspondence:
Zi Chen
e-mail: zi.chen@dartmouth.edu

Electronic supplementary material is available online at rs.figshare.com.

THE ROYAL SOCIETY PUBLISHING

How the embryonic chick brain twists

Zi Chen[1,2], Qiaohang Guo[3,4], Eric Dai[1], Nickolas Forsch[1,5] and Larry A. Taber[1]

[1]Department of Biomedical Engineering, Washington University, St Louis, MO 63130, USA
[2]Thayer School of Engineering, Dartmouth College, Hanover, NH 03755, USA
[3]School of Materials Science and Engineering, Fujian University of Technology, Fuzhou 350108, People's Republic of China
[4]Fujian Provincial Key Laboratory of Advanced Materials Processing and Application, Fuzhou 350108, People's Republic of China
[5]Department of Bioengineering, University of California at San Diego, La Jolla, CA 92093, USA

ZC, 0000-0001-5927-0249

During early development, the tubular embryonic chick brain undergoes a combination of progressive ventral bending and rightward torsion, one of the earliest organ-level left–right asymmetry events in development. Existing evidence suggests that bending is caused by differential growth, but the mechanism for the predominantly rightward torsion of the embryonic brain tube remains poorly understood. Here, we show through a combination of *in vitro* experiments, a physical model of the embryonic morphology and mechanics analysis that the vitelline membrane (VM) exerts an external load on the brain that drives torsion. Our theoretical analysis showed that the force is of the order of 10 micronewtons. We also designed an experiment to use fluid surface tension to replace the mechanical role of the VM, and the estimated magnitude of the force owing to surface tension was shown to be consistent with the above theoretical analysis. We further discovered that the asymmetry of the looping heart determines the chirality of the twisted brain via physical mechanisms, demonstrating the mechanical transfer of left–right asymmetry between organs. Our experiments also implied that brain flexure is a necessary condition for torsion. Our work clarifies the mechanical origin of torsion and the development of left–right asymmetry in the early embryonic brain.

1. Introduction

Morphogenesis, the generation of biological form [1], has been studied for centuries. In his classic book, *On growth and form* [2], Thompson suggests that the form of an organism (and its changes) can be 'explained by the interaction or balance of forces', calling attention to the need for understanding the mathematical and physical aspects of biological growth and morphogenesis. While modern developmental biologists have mostly focused on the genetic and molecular aspects of development, the search for mathematical and mechanical principles of morphogenesis has never ceased and is currently being revived [3–10].

The transformation of a straight configuration to a chiral shape is ubiquitous in natural and engineered systems [5,11–13]. Although the physical and molecular mechanisms in morphogenesis have been studied for centuries [1–3,5–8,12,14], except for a few studies [15–17], the roles of mechanical forces in early brain morphogenesis are still poorly understood. In particular, the fundamental mechanism underlying the torsion of the embryonic brain [18], one of the earliest morphogenetic events of left–right (L–R) asymmetry in the embryo, remains elusive. Significant birth defects can result when the process of L–R specification is perturbed, including *situs inversus* (inversion of the positions of visceral organs), isomerism (mirror image symmetry of bilaterally asymmetric tissues) and heterotaxia (random and independent occurrence of laterality defects in different tissues) [19].

At Hamburger & Hamilton [20] (HH) stage 10 (after approx. 33 h of incubation), the neural tube of the chick embryo is nearly straight. The anterior

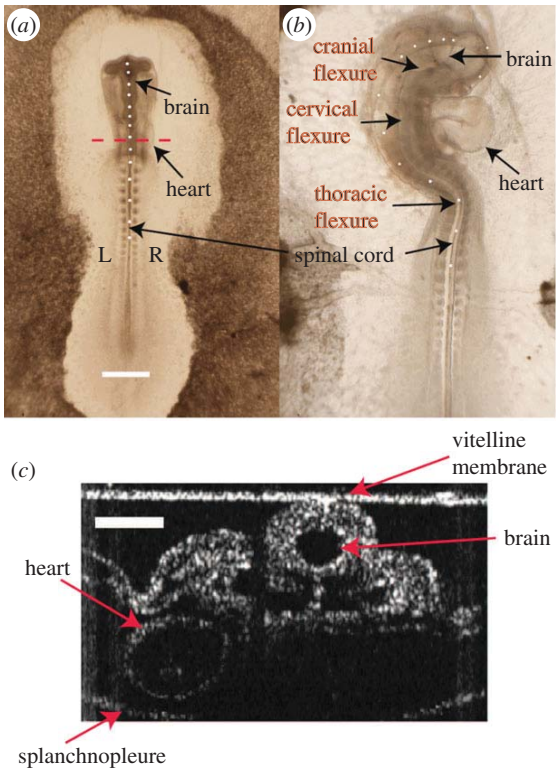

Figure 1. Flexure and torsion in early brain development of a normal chick embryo (dorsal view). (*a*) Dorsal view of nearly straight brain tube at Hamburger and Hamilton (HH) stage 11. The white dots are virtual markers on the neural tube for visualizing the large deformation during flexure and torsion. Scale bar, 1 mm. (*b*) Dorsal view of same embryo 20 h later featuring flexure and torsion in the brain tube. The embryonic brain turns rightward, so that its left side lies on the substrate. (*c*) Transverse section of HH stage 12 chick embryo obtained by optical coherence tomography; the heart is on the embryonic right, the VM is dorsal to the embryo, whereas the SPL is ventral to the embryo. L, left; R, right. Scale bar, 0.5 mm.

part of the neural tube expands to create the primitive brain tube (figure 1*a*), which then undergoes shape changes that involve ventral bending (flexure) and rightward twisting (torsion). These shape changes eventually alter the position of the embryo relative to the yolk [21].

Flexure is considered to consist of two main phases. First, the embryo bends about a transverse axis through the midbrain (cranial flexure, figure 1*b*), followed by bending from the hindbrain to the spinal cord (cervical flexure). During torsion, the brain tube twists rightward, so that the left side of the brain rests upon the yolk, whereas the posterior part of the neural tube (future spinal cord) maintains its original orientation (electronic supplementary material, movie S1). Flexure and torsion occur almost concurrently in chick embryos, as torsion first appears almost simultaneously with the beginning of cranial flexure and continues as flexure progresses. Also noteworthy is the fact that torsion usually occurs, so that the head turns rightward. Indeed, axial rotation is one of the earliest morphogenetic events of L–R asymmetry in the embryo [18], immediately following the asymmetric looping of the heart. A third flexure, termed 'thoracic flexure', immediately precedes torsion, bending the embryonic neural tube in a direction opposite to cranial and cervical flexures.

Previous studies have suggested that bending of the brain tube could be attributed in part to differential growth [22], but the biomechanical mechanism of brain torsion remains poorly understood. Interestingly, the heart almost always loops in the same direction (to the right side) that the brain twists, leading some researchers to speculate that the looping heart affects the direction of brain torsion [23,24]. Nevertheless, little direct evidence exists, and the mechanical origin of brain torsion remains elusive.

Here, we use experiments in developing chick embryos and a physical model to show that (i) the vitelline membrane (VM) exerts a mechanical load that causes the brain tube to twist as it bends, (ii) the direction of the looping heart determines the direction of torsion, and (iii) brain flexure is a necessary condition for torsion.

2. Results

2.1. The vitelline membrane applies the compressive load necessary for torsion

In a normal HH11 chick embryo (after approx. 40–45 h of incubation), the embryonic brain tube has not yet begun to twist (figure 1*a*). After around 20 h of cultivation (to approx. HH stage 16), the brain tube is bent and twisted rightward, whereas the spinal cord is still in its original orientation (figure 1*b*). A thin membrane called the VM, which is under tension, constrains the embryo on its original dorsal side, and the splanchnopleure (SPL) membrane constrains the heart on the ventral side (figure 1*c*). Studies have shown that the SPL membrane is a primary cause of torsion of the looping heart [25].

To determine whether the VM, an often-overlooked developmental structure, plays a mechanical role in brain morphogenesis, we removed this membrane before the onset of torsion. More specifically, the VM was cut from the anterior end of the embryo to the spinal cord at the point of the thoracic flexure (figure 2*b*). Notably, embryos (starting from stage HH11, as shown in figure 2*a*; $n = 12$, where n is the number of embryos tested) cultivated for 27 h to HH stage 17 without the dorsal constraint of the VM exhibited considerably less torsion than control embryos. For example, the torsional angle near the eyes ≈34 degrees in such an embryo shown in figure 2*b* (see electronic supplementary material, texts and figure S3 for the method of measuring the torsional angle) when compared with the torsional angle ≈88 degrees in a control embryo (figure 2*d*). Furthermore, when we lowered the fluid level in the Petri dish to apply surface tension to the embryo (i.e. when the embryonic brain is exposed to the air–fluid interface it becomes subjected to the fluid surface tension) [26], we found that the brain instantaneously twisted rightward (figure 2*c* and electronic supplementary material, movie S2), with degrees of torsion similar to the control embryos (e.g. the one in figure 2*d*). In addition, embryos with the VM removed at HH11 and subjected to surface tension from the culture media showed a similar degree of torsion after another 20 h of cultivation (figure 2*e*) in that case the surface tension again replaces the mechanical role of the VM in inducing normal torsion. Taken together, these results suggest that the VM applies compressive loads necessary for normal brain

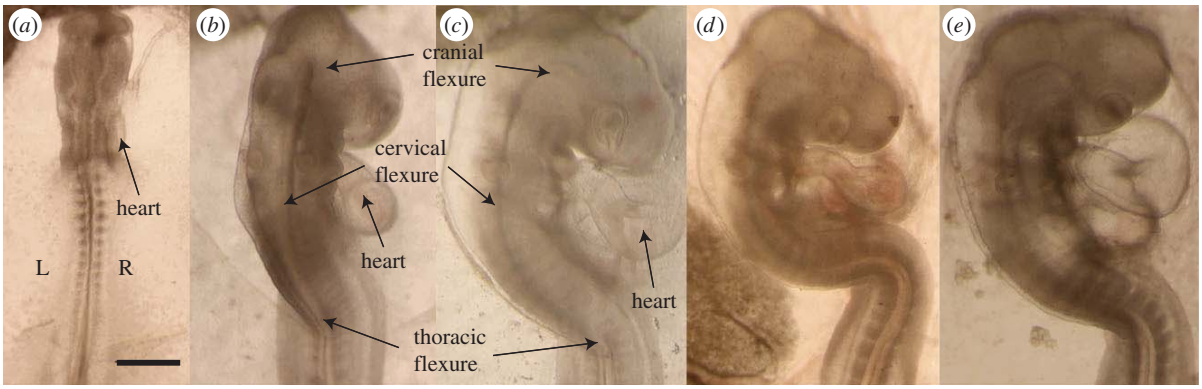

Figure 2. Effects of external forces on brain torsion (dorsal view). (*a*) Embryo with a nearly straight brain tube and VM removed at HH stage 11. (*b*) Same embryo 27 h later showing a relatively small amount of rightward torsion. (*c*) Same embryo under surface tension immediately gained significant additional brain torsion (see electronic supplementary movie). (*d*) Control embryo with normal brain torsion at a comparable stage. (*e*) Embryo with VM removed at HH stage 11, shown after approximately 20 h of cultivation under fluid surface tension. Brain torsion is normal, suggesting that the fluid surface tension replaced the mechanical forces formerly supplied by the VM. Scale bar, 1 mm.

torsion and that surface tension can serve as an analogous and alternative driving force for such torsion.

2.2. The direction of the looping heart determines the direction of the twisting brain

In general, the embryonic chick brain twists in the same direction that the heart loops [23], leading researchers to speculate that the looping direction of the heart affects the direction of brain torsion [23,24,27]. To test this hypothesis, we pushed the rightward-looped heart (figure 3*a*) to the left in stage 11–12 embryos (figure 3*b*). The SPL held the heart in this position. After 17–25 h of cultivation, the brains in all of these embryos ($n = 16$) twisted abnormally to the left (figure 3*c*). These results support the hypothesis that the twisting direction of the brain tube is determined by the direction of heart looping. When these experiments were repeated with surface tension replacing the mechanical role of SPL, the embryos still all turned leftward ($n = 7$), implying a fundamental mechanical basis for the transfer of chirality between the heart and brain of the embryonic chick.

We tried to repeat these experiments in embryos at later stages (e.g. HH stage 13 or beyond) in which brain torsion was already significant. At the most advanced stage of development, however, the displaced heart did not remain on the left side, and all the embryonic brains still turned rightward (figure 3*d–f*). A detailed examination showed that for a stage 13 embryo (or older), the mechanically displaced heart gradually returned to the right side (within a minute or two) as the heart beat (electronic supplementary material, movie S3), and normal brain torsion resumed. Taken together, these results suggest that the direction of heart looping determines the direction of brain torsion, with rightward looping inducing rightward brain torsion, and leftward looping inducing leftward brain torsion. Because the heart predominantly loops to the right side (more than 99% in ovo [23]), it follows that the embryonic brain usually twists rightward.

To further understand how the heart affects brain torsion, we constructed a physical model (see Methods). The model is based on simplified geometry for a chick embryo at HH stage 14–17 without the VM (figure 2*b*). The embryonic brain is modelled as a curved rod with an elliptical cross section and prescribed intrinsic curvatures (for simplicity, we have just used a circular rod with the same magnitude of the radius, figure 4*a*,*b*). The heart is modelled as another curved rod looped towards the right side and constrained by contact with a block representing the SPL (figure 4*b*,*c*). A mechanical load is applied at the top of the physical model by a coverslip representing the VM (figure 4*d*), which is moved downward to compress the brain. Figure 4*d* shows a slight rightward twisting of the chick embryo model (with the heart looped rightward) subjected to a moderate mechanical load along the gravity direction from the top. Both the physical model and the embryo exhibit similar rightward twisting when the heart loops to the right side, in support of our hypothesis. Figure 4*e* shows the deformed shape of the physical model when subjected to a larger force from the coverslip than in figure 4*d*, exhibiting a more significant rightward torsion than in figure 4*d*, comparable to that in a HH 14 chick embryo.

Ideally, the model without the heart is L–R symmetric, and the brain bends without twisting. With the heart looped to the right side, however, the embryo becomes L–R asymmetric, and the brain tube twists rightward (figure 4*d*,*e*). On the other hand, if the heart loops to the left (electronic supplementary material, movie S4) or is pushed to the left side (figure 3*a–c*), then the brain twists leftward. The reason for this behaviour is that the ventral motion of the heart is constrained by the SPL, causing the heart to push the brain tube leftward at the point where these organs are connected. This force exerts a torque relative to the fixed spinal cord, causing the brain to twist rightward relative to its body axis. Simply put, the presence of the heart breaks the symmetry and causes the brain to twist asymmetrically relative to the fixed spinal cord region when subjected to external forces from either the VM or surface tension. These results are consistent with our previous experiments, lending support to the hypotheses that the VM applies a mechanical load necessary for brain torsion, whereas the looping direction of the heart determines the chirality of the twist.

2.3. Brain flexure is another requisite condition for torsion

Inspired by the work of Männer *et al.* [28], we implanted an eyelash into the lumen of the brain tube to suppress flexure in order to study the relationship between brain bending

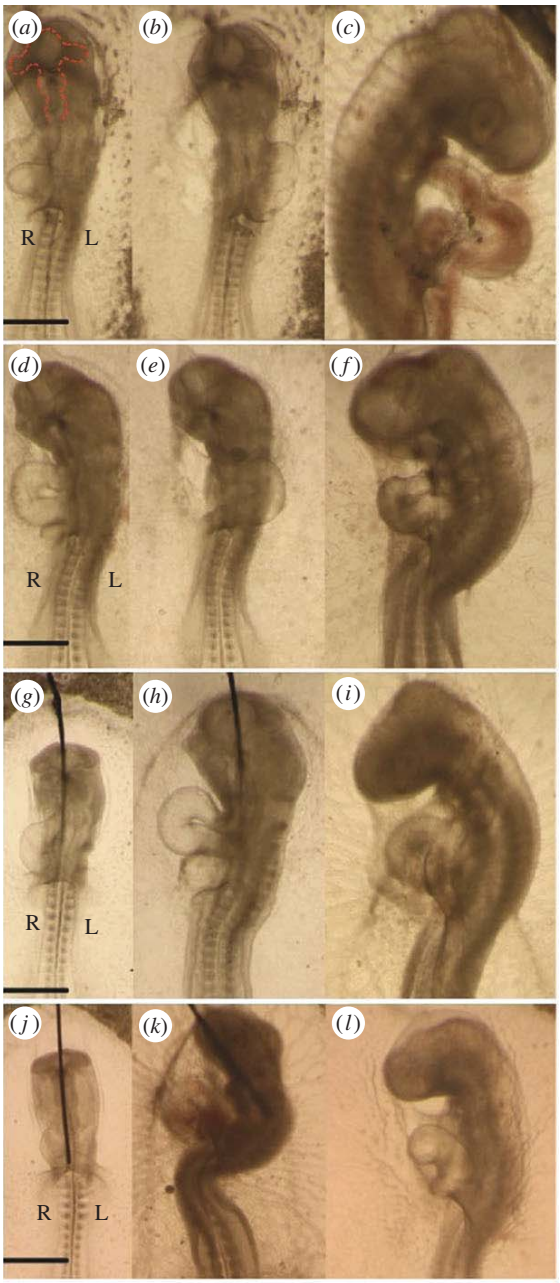

Figure 3. Effects of heart-looping direction and brain flexure on torsion (ventral view). (*a*) HH stage 12 embryo with heart (H) looped normally to the right side. (*b*) Same embryo with heart pushed to the left side. Surface tension is immediately applied to keep the heart on the left. (*c*) Same embryo 20 h later; the brain tube twists leftward. (*d*) HH stage 13 embryo with the head rotated partially rightward. (*e*) Same embryo with heart pushed to the left side, and surface tension immediately applied. (*f*) Same embryo 18 h later. The brain turns right as in a normal embryo. (*g*) Chick embryo at HH stage 11 with eyelash implanted in the brain tube to suppress flexure. (*h*) Same embryo 18 h later shows little brain torsion. (*i*) Normal embryo at a comparable stage to the manipulated embryos in (*b*) and (*h*). (*j*) Chick embryo at HH stage 10+ with an eyelash implanted in the brain tube (not reaching the first somite). (*k*) Same embryo 20 h later exhibiting comparable amount of torsion to control. (*l*) Control embryo (an eyelash was inserted in the brain tube at HH stage 10+ and immediately removed) with normal rightward torsion. Scale bar, 1 mm.

and torsion. The eyelash was implanted in the brain tube at HH stage 11 (figure 3*g*, $n = 7$) to reach at least the second somite, and the embryo was cultivated for approximately

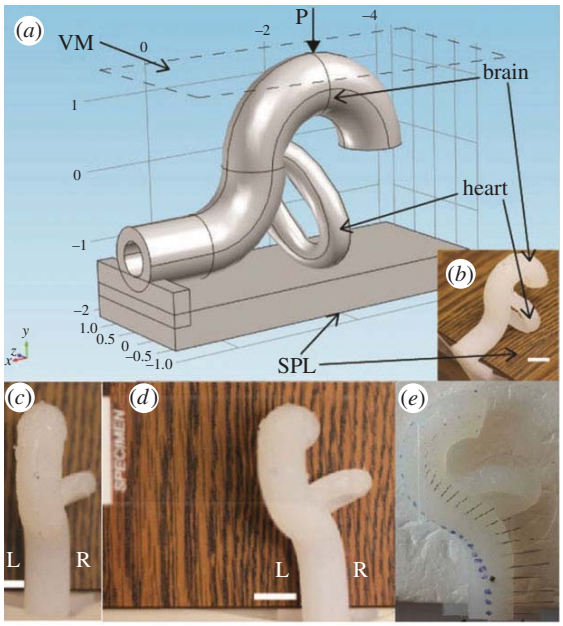

Figure 4. Physical model of embryonic brain torsion. (*a*) Simplified geometry of a chick embryo at HH stage 14–17 in computer-aided design (Comsol MultiPhysics). (*b*) Silicone elastomer casted physical model of simplified geometry. Scale bar, is 1 cm in all subpanels. (*c*) Dorsal view of model with heart on right side before downwards force application by coverslip. (*d*) Dorsal view of model following downwards force application by coverslip, with brain beginning to twist rightwards. (*e*) Model after further force application, with brain twisted more drastically rightwards. Fiducial markers (marks and pins), used to visualize torsion, are also shown.

18 h. Much less torsion of the brain tube was observed (figure 3*h*; torsional angle ≈35 degrees) when compared with an unperturbed embryo (figure 3*i*; torsional angle ≈88 degrees) or a control embryo (with an eyelash implanted and removed immediately at HH11) cultivated to a similar stage (figure 3*l*; torsional angle ≈88 degrees). These results suggest that the development of curvatures in the brain tube is also a necessary condition for normal brain torsion to occur.

It is noteworthy that, in addition to the cranial and cervical flexures, a third flexure develops in the neural tube. This flexure occurs posterior to cervical flexure and near the anterior part of the spinal cord, and bends the embryo in a direction opposite to the cranial and cervical flexures (figures 1*b* and 2*b*,*c*). This otherwise overlooked flexure, namely the 'thoracic flexure', is still visible in embryos with the VM removed (figure 2*b*,*c*), as well as in rat and mouse embryos [27,29]. We found that the thoracic and cervical flexures play an important role in the development of brain torsion. When these flexures were suppressed by implantation of an eyelash much stiffer than the embryonic tissues, brain torsion was also significantly suppressed (figure 3*h*). However, when only the cranial flexure was suppressed by an implanted eyelash not reaching the first somite (figure 3*j*, $n = 7$), the embryo still turned rightward (figure 3*k*), exhibiting a comparable degree of torsion (torsional angle ≈83 degrees) to a normal embryo (figure 3*i*; torsional angle ≈88 degrees) or a control embryo (figure 3*l*). Therefore, the development of thoracic and cervical flexures constitute a requisite condition for normal brain torsion, but not the other way around, i.e. even if brain torsion was dramatically reduced (figure 2*b*), the magnitudes of the flexures were not significantly affected.

2.4. Estimation of the magnitude of the force

The VM, acting as a mechanical boundary for the growing embryonic brain tube, was shown to be a necessary structure for the twisting of the brain. In particular, the passive downward force of the VM was shown to be fundamental in this role: the brain no longer twisted to a normal degree when the VM of the embryo was removed, but could be made to twist to control levels through the application of surface tension force from lowering culture fluid levels. Because the surface tension of water at the ambient temperature is $72.01 \pm 0.1\,\mathrm{mN\,m^{-1}}$ [30], and the contact length is on the order of millimetres, the force

$$F \approx 72 \times 10^{-3}\,\mathrm{N\,m^{-1}} \times 10^{-3}\,\mathrm{m} \approx 10^{-5}\,N = 10\,\mu\mathrm{N}.$$

Thus, we determine that the VM exerts a force of approximately 10 μN on the HH 14–17 embryo. Alternatively, F can be estimated as by considering the balance of the torque

$$F \times 2R \approx GJ\tau = \frac{GJ}{2R}, \tag{2.1}$$

where R is the radius of curvature for all flexures (assuming all flexures have the same curvature), G is the shear modulus and J is the cross-sectional polar moment of inertia. The torsion is $\tau = \pi/2/(\pi R) = 1/(2R)$ when the embryo is twisted by $\pi/2$. Therefore,

$$F \approx \frac{GJ}{4R^2} = \frac{G(\pi d^4/32)}{4R^2}.$$

Using the following estimated values: $G \approx 200$ Pa, $d \approx 1.8$ mm and $R \approx 1.5$ mm, it follows that $F \approx 10$ μN, consistent with the previous estimated value using the surface tension.

3. Discussion

In this study, we demonstrated through experiments and a physical model that the combination of the rightward looping heart and the physical constraint of the VM are necessary and sufficient conditions for the rightward torsion of the ventrally flexed brain tube of the chick embryo.

The cervical and thoracic flexures were also shown to be necessary conditions for the development of torsion. When these flexures were allowed to develop normally, torsion also proceeded normally; however, when these flexures were suppressed through the axial implantation of an eyelash, torsion was drastically attenuated. We can verify that the insertion of the eyelashes forcibly suppresses the curvature of the embryonic body by comparing the relative bending stiffnesses of the two objects. The linear elastic modulus of the embryonic midline structures at HH 10 has been measured at 2.4 ± 0.1 kPa [31], whereas the linear elastic modulus of human hair is approximately 9.5 GPa [32]. The bending rigidity of a circular rod is

$$EI \propto Ed^4,$$

where E is the linear elasticity, I is the moment of inertia and d is the beam diameter. Therefore,

$$\frac{(EI)_{\mathrm{eyelash}}}{(EI)_{\mathrm{embryo}}} \approx 10^6 \times \left(\frac{d_{\mathrm{eyelash}}}{d_{\mathrm{embryo}}}\right)^4 \approx 10^2 \gg 1,$$

where $d_{\mathrm{eyelash}}/d_{\mathrm{embryo}} \approx 0.1$. In other words, the bending rigidity of the inserted eyelash is two orders of magnitude higher than the embryo and thus effectively suppresses the flexure of the embryonic brain.

From a broader perspective, spontaneous chiral structures are ubiquitous in natural and engineering structures, from the DNA double helix to looping guts [5], from chiral seed pods [11] and plant tendrils [12,33,34] to strained multilayer composites [11,13,35,36] and curly hair [37], where a variety of mechanical or biophysical mechanisms are operating. Morphogenesis is a complex biophysical process, whereby mechanical cues interact with molecular mechanisms in an exquisitely orchestrated fashion to regulate the shaping of functional biological form [1,3,7]. Within the transforming growth factor TGF-β family, *lefty* and *nodal* are known to play important roles in the determination and maintenance of L–R asymmetry [38,39]. While gene expression and molecular signalling are certainly central to embryonic development, the role of mechanical forces in morphogenesis has been increasingly acknowledged [3,5–8]. For example, Savin *et al*. [5] discovered that forces generated by different growth rates between the gut tube and the adjacent dorsal mesenteric sheet drive the morphogenesis of gut looping. More recently, Shyer *et al*. revealed the role of mechanical stresses in the formation of villi in the gut [8]. Forces extrinsic to the primitive heart tube also are important players during cardiac looping [14,26,40,41]. Results from these studies suggest that the SPL plays a mechanical role in facilitating cardiac torsion that may be similar to the role of the VM in inducing brain torsion. A more recent study implies that both differential contractility and stress-dependent growth play key roles in early brain morphogenesis [42].

Axial rotation of the neural tube is among the earliest tissue-level events that breaks LR symmetry in the developing embryos [18], following the rightward looping of the heart. In amniote embryos, such as chicken and mice [19], brain torsion typically begins a few hours after cardiac looping begins. Severe defects can result when the process of LR specification is perturbed, including situs inversus (inversion of the positions of visceral organs), isomerism (mirror image symmetry of bilaterally asymmetric tissues) and heterotaxia (random and independent occurrence of laterality defects in different tissues) [19].

The detailed mechanisms of axial rotation may vary because of different amounts of yolk present in different species. In yolk-less mammalian embryos, such as those of a rat or mouse, the embryonic axis first develops a 'U' shape with the outer curvature of the embryo being ventral and the inner curvature being dorsal [43]. Then, at a species-dependent stage (from 10.5 to 11.5 days in the rat and from 8.5 to 9.5 days in the mouse), the embryo rotates about its axis so that the dorsoventral orientation of the curvature inverts. During this process, the head turns rightward as in the avian embryo. In this case, however, the rotational angle is 180 degrees, in contrast to the 90-degree turn in yolk-rich avian embryos, where the constraint of the yolk prevents further rotation. The fundamental mechanism behind axial rotation in mammalian embryos is still poorly understood. It has been suggested that differential growth owing to asymmetric cell proliferation causes this rotation. Some investigators have speculated that the extraembryonic membranes and the beating heart play important roles in regulating axial rotation [27,29,43]. However, the contributions of these factors to axial rotation and their interplay require further study before definitive conclusions can be drawn.

In normal chick embryos, the brain tube twisted into a left-handed helix just after the heart loops into a left-handed

helix [28]. In a sense, this process can be considered as a transfer of chirality or LR asymmetry, from the heart to the brain tube through mechanics. Following the first phase of cardiac looping (c-looping), brain torsion in turn ensures the normal helical looping of the heart during the subsequent s-looping [41]. This type of transfer of chirality between two co-developing organs at the same length scale has not previously been examined in detail, although the transfer of chirality from microscopic-to-macroscopic scale in plant tendrils has recently been studied [34]. It is worth noting that in murine embryos, the LR asymmetry of the developing heart might also affect axial rotation of the embryo [43]. It has been suggested that the neural tube itself may not be the motor that drives torsion; instead, the coordinated activity of somites may play a role [29]. In biological systems, chirality can transfer from the microscopic level (such as in the cytoskeleton) [44] to the cell, tissue and organism level [45], but whether this principle applies to chirality generation in embryonic axial rotation remains unknown.

It also remains to be examined how mechanical and molecular mechanisms interact and coordinate to regulate morphogenesis. For example, Manca *et al*. [46] recently discovered that nerve growth factor (NGF) regulates axial rotation in chick embryos, as injection of an anti-NGF antibody induces a dose-dependent inversion of rotation direction. Specifically, a high dose causes a remarkable change in the direction of rotation to the left side (reversed torsion). Nevertheless, it is unclear whether NGF regulation works directly or indirectly on axial rotation in chick embryos, because misdirection of heart looping can also reverse the rotation direction of the brain.

Moreover, researchers have proposed that the axial rotation in mammalian embryos is correlated with asymmetry in the developing heart [43] and asymmetric mitotic activity in the developing neural tube [47]. Abnormal looping direction in the heart often occurs concurrently with reversed turning of the embryo [48], suggesting the correlation between heart torsion and axial rotation directions may also exist in mammalian embryos.

However, the role of mechanical stresses in axial rotation of mammalian embryos remains poorly understood. Presumably, the 180-degree turn in murine embryos should be more difficult than the 90-degree turn in avian embryos. Nevertheless, axial rotation in mouse embryos finishes at the 13-somite stage, whereas in chick embryos, this process is not completed until HH stage 20 with around 40–43 somites. We speculate that mechanical forces also play an important role in the axial rotation of murine embryos. Possibly involved are the mechanical factors related to constraints from the extraembryonic membranes and the asymmetrically looped heart, because the heart also normally loops to the right and the head turns rightward in normal murine embryos. Notably, both thoracic flexure and cranial flexure are even more significant in rodents before the axial rotation starts (evidenced by the 'U' shape), which suggests that some mechanical mechanism similar to that in avian embryos could be operating. Further important insights can be gained by studying embryos with defects in axial rotation, for example, chick embryos with misexpression of the *Cerberus* (*cCer*) gene (related genes include *Xenopus Ceberus* and mouse *mCer-1*/*mCer-l*) [49], mutant mouse embryos such as *fur* [50] and *no turning* (*nt*) [51], or embryos lacking in the gene *rotatin* [19].

Collectively, our study shows that normal brain torsion in the chick embryo requires at least three mechanical conditions: pressure exerted by the VM; rightward looping of the heart that dictates the brain torsion direction and appropriate neural tube flexures, especially cervical and thoracic flexures. Our experiments and simulations confirm that the torsion direction is determined by the heart-looping direction, demonstrating a transfer and amplification of L–R asymmetry through mechanics. In return, the increasing brain torsion may provide the mechanical forces necessary for the normal morphogenesis of cardiac s-looping [41], such that these two torsional morphogenic events reinforce each other to ensure normal development. Furthermore, we found that the traditionally overlooked thoracic flexure, together with cervical flexure, plays a key role in inducing brain torsion. By considering the balance of torque, the force from the VM is estimated to be in the order of 10 micronewtons, consistent with the estimate made by calculating the alternative force from the fluid surface tension. This work clarifies the mechanical origins of brain torsion and the associated propagation of L–R asymmetry in avian embryos, thus providing a new biomechanical example recapitulating Thompson's view of biological form as a 'diagram of forces' [2]. Our study also raises questions about how mechanical and biomolecular mechanisms co-regulate morphogenesis and how they have evolved or been preserved across species, inviting further investigations.

4. Methods

4.1. Embryo culture

Fertilized White Leghorn chicken eggs were incubated in a humidified atmosphere at 38°C for 40–48 h to yield embryos at Hamburger and Hamilton (HH) stages 11–13 [25]. Whole embryos were harvested from the eggs using a filter paper carrier method [40]. Each embryo was then placed either dorsal or ventral side up in a 35 mm culture dish, completely submerged under a thin layer of liquid culture media, and then incubated at 38°C in 95% O_2 and 5% CO_2. To preserve humidity, several drops of deionized water were put into the bag containing the culture dish before placing the sealed bag into the incubator. In control embryos, all membranes were kept intact, thus preserving the normal stresses present in the tissue. For mechanical perturbations, microsurgical operations were performed, using fine glass needles. The embryos were subjected to surface tension forces when exposed to air [40]; therefore, by controlling the air–medium interface, the surface tension can be tuned (electronic supplementary material, movie S2). Moreover, the measurement of the torsional angle from the optical coherent tomograph images is illustrated in extended data (figure 1). Despite the consistent results from experiments with embryos that we have drawn our conclusions on, we recognize the limitations set by the paper culture method used, because abnormalities can occur especially when the development of blood vessels is hindered by the surrounding filter paper. Abnormal growth, such as underdevelopment or observed decay in tissue health, is expected and can occur for various reasons. As such, abnormal embryos were often excluded from the study because they cannot ensure a control in variables beyond the variable being perturbed, such as the removal of the VM. As with most experiments with embryos using the paper culture method, embryonic health is determined through observation. Similarly, experiments that investigated the chirality of the brain torsion owing to the direction of the looping heart could be expanded

upon with more control experiments, e.g. removing the heart completely or grafting the heart to the other side of the embryo. However, such drastic perturbations to the embryo could affect the viability enough to discredit any observations that result from the perturbations, as opposed to morphological changes in response to altered developmental mechanisms; thus, such instances were not included in the study. Although some minor developmental abnormalities could still occur occasionally, for example, the abnormal degree of trunk torsion (near the thoracic flexure) as shown in figures 2*d* and 3*k*, these aberrations occur later than the investigated stages and do not interfere with the objectives of this study (the origins of the embryonic brain torsion and the chirality).

4.2. Imaging

Bright-field images were acquired, using a dissecting microscope (Leica MZ8). A Thorlabs (Newton, NJ) optical coherence tomography system with attached Nikon FN1 microscope was used to acquire cross-sectional image stacks of live embryos. Images were obtained in a $3\,\text{mm} \times 10 \times 3\,\text{mm}$ scanning domain, then processed in ImageJ. The image of the physical model was taken with a digital single-lens reflex camera (EOS Rebel T3i).

4.3. Physical model

To further illustrate the torsion mechanism, we created a physical model of the embryo. A three-dimensional model of the embryonic morphology was developed in commercial software, COMSOL MultiPhysics. A negative mould of the model was then developed in Rhino 5 by applying Boolean subtraction of the three-dimensional model of the chick embryo from a larger block and splitting the resulting block into three attachable blocks. Following this, we used a three-dimensional printer (Makergear M2, made by MakerBot, Inc.) loaded with 1.75 mm acrylonitrile butadiene styrene filament to three-dimensional print the negative mould. To cast the mould, we used a fast curing, soft silicone elastomer (EcoFlex 00-50, purchased from Smooth-On, Inc.). We measured and combined equal parts of the two elastomer agents at room temperature, approximately 7.0 g of each agent, and poured the mixture into the mould slowly and evenly from a single point to minimize air bubble formation. We then clamped the mould shut and allowed the EcoFlex to cure for 12 h at room temperature.

Authors' contribution. Z.C. conceived of the study, carried out part of biophysical experiments, theoretical analysis, data analysis, participated in the design of the study and drafted the manuscript; Q.G. carried out part of the biophysical experiments; E.D. made the physical model and carried out data analysis, and helped draft the manuscript. N.F. helped with the biophysical experiments and data analysis; L.A.T. participated in the design of the study and helped draft the manuscript. All authors gave final approval for publication.

Competing interests. The authors declare no competing interests.

Funding. Z.C. acknowledges the support by the Society in Science-Branco Weiss fellowship, administered by ETH Zurich. Q.G. acknowledges the support from National Natural Science Foundation of China (grant no. 11102040) and Projects of International Cooperation and Exchanges NSFC (grant no. 11201001044). L.A.T. acknowledges the support from NIH grant nos. R01 GM075200 and R01 NS070918.

Acknowledgements. The authors thank Sihao Chen, Jayne Hanlin, Dr Ruth Okamoto, Philip Bayly, David Beebee, Howard Stone and Matthew Martin for comments.

References

1. Taber LA. 1995 Biomechanics of growth, remodeling, and morphogenesis. *Appl. Mech. Rev.* **48**, 487–545. (doi:10.1115/1.3005109)
2. Thompson DW. 1971 *On growth and form*. Cambridge, UK: Cambridge University Press.
3. Gjorevski N, Nelson CM. 2010 The mechanics of development: models and methods for tissue morphogenesis. *Birth Defects Res. C Embryo Today* **90**, 193–202. (doi:10.1002/bdrc.20185)
4. Davidson LA. 2011 Embryo mechanics: balancing force production with elastic resistance during morphogenesis. *Curr. Top. Dev. Biol.* **95**, 215–241. (doi:10.1016/B978-0-12-385065-2.00007-4)
5. Savin T, Kurpios NA, Shyer AE, Florescu P, Liang H, Mahadevan L, Tabin CJ,. 2011 On the growth and form of the gut. *Nature* **476**, 57–62. (doi:10.1038/nature10277)
6. Ambrosi D *et al.* 2011 Perspectives on biological growth and remodeling. *J. Mech. Phys. Solids* **59**, 863–883. (doi:10.1016/j.jmps.2010.12.011)
7. Wyczalkowski MA, Chen Z, Filas BA, Varner VD, Taber LA. 2012 Computational models for mechanics of morphogenesis. *Birth Defects Res. C* **96**, 132–152. (doi:10.1002/bdrc.21013)
8. Shyer AE, Tallinen T, Nerurkar NL, Wei Z, Gil ES, Kaplan DL, Tabin CJ, Mahadevan L. 2013 Villification: how the gut gets its villi. *Science* **342**, 212–218. (doi:10.1126/science.1238842)
9. Brunet T *et al.* 2013 Evolutionary conservation of early mesoderm specification by mechanotransduction in Bilateria. *Nat. Commun.* **4**, 282. (doi:10.1038/ncomms3821)
10. Papastavrou A, Steinmann P, Kuhl E. 2013 On the mechanics of continua with boundary energies and growing surfaces. *J. Mech. Phys. Solids* **61**, 1446–1463. (doi:10.1016/j.jmps.2013.01.007)
11. Armon S, Efrati E, Kupferman R, Sharon E. 2011 Geometry and mechanics in the opening of chiral seed pods. *Science* **333**, 1726–1730. (doi:10.1126/science.1203874)
12. Gerbode SJ, Puzey JR, McCormick AG, Mahadevan L. 2012 How the cucumber tendril coils and overwinds. *Science* **337**, 1087–1091. (doi:10.1126/science.1223304)
13. Chen Z, Majidi C, Srolovitz DJ, Haataja M. 2011 Tunable helical ribbons. *Appl. Phys. Lett.* **98**, 011906. (doi:10.1063/1.3530441)
14. Shi YF, Yao J, Young JM, Fee JA, Perucchio R, Taber LA. 2014 Bending and twisting the embryonic heart: a computational model for c-looping based on realistic geometry. *Front. Physiol.* **5**, 297. (doi:10.3389/fphys.2014.00297)
15. Xu G, Knutsen AK, Dikranian K, Kroenke CD, Bayly PV, Taber LA. 2010 Axons pull on the brain, but tension does not drive cortical folding. *J. Biomech. Eng.* **132**, 071013. (doi:10.1115/1.4001683)
16. Filas BA, Oltean A, Beebe DC, Okamoto RJ, Bayly PV, Taber LA. 2012 A potential role for differential contractility in early brain development and evolution. *Biomech. Model. Mechanobiol.* **11**, 1251–1262. (doi:10.1007/s10237-012-0389-4)
17. Tallinen T, Chung JY, Biggins JS, Mahadevan L. 2014 Gyrification from constrained cortical expansion. *Proc. Natl Acad. Sci. USA* **111**, 12 667–12 672. (doi:10.1073/pnas.1406015111)
18. Fujinaga M, Hoffman BB, Baden JM. 1995 Axial rotation in rat embryos: morphological analysis and microsurgical study on the role of the allantois. *Tetratology* **51**, 94–106. (doi:10.1002/tera.1420510208)
19. Faisst AM, Alvarez-Bolado G, Treichel D, Gruss P. 2002 *Rotatin* is a novel gene required for axial rotation and left–right specification in mouse embryos. *Mech. Dev.* **113**, 15–28. (doi:10.1016/S0925-4773(02)00003-5)
20. Hamburger V, Hamilton HL. 1992 A series of normal stages in the development of the chick embryo. *Dev. Dyn.* **195**, 231–272. (doi:10.1002/aja.1001950404)
21. Patten BM. 1920 *The early embryology of the chick*. Philadelphia, PA: P. Blakiston's Son and Co.
22. Takamatsu T, Fujita S. 1987 Growth of notochord and formation of cranial and mesencephalic flexures in chick embryo. *Dev. Growth Differ.* **29**, 497–502. (doi:10.1111/j.1440-169X.1987.00497.x)

23. Hoyle C, Brown NA, Wolpert L. 1992 Development of left/right handedness in the chick heart. *Development* **115**, 1071–1078.
24. Waddington CH. 1937 The dependence of head curvature on the development of the heart in the chick embryo. *J. Exp. Biol*. **14**, 229–231.
25. Nerurkar NL, Ramasubramanian A, Taber LA. 2006 Morphogenetic adaptation of the looping embryonic heart to altered mechanical load. *Dev. Dyn*. **235**, 1822–1829. (doi:10.1002/dvdy.20813)
26. Voronov DA, Taber LA. 2002 Cardiac looping in experimental conditions: effects of extraembryonic forces. *Dev. Dyn*. **224**, 413–421. (doi:10.1002/dvdy.10121)
27. Miller SA, White RD. 1998 Right–left asymmetry of cell proliferation predominates in mouse embryos undergoing clockwise axial rotation. *Anat. Rec*. **250**, 103–108. (doi:10.1002/(SICI)1097-0185(199801)250:1<103::AID-AR10>3.0.CO;2-S)
28. Männer J, Steding G, Seidl W. 1993 Correlation between the embryonic head flexures and cardiac development: an experimental study on chick embryos. *Anat. Embryol*. **188**, 269–285. (doi:10.1007/BF00188218)
29. Deuchar EM. 1975 Further observations on axial rotation in rat embryos. *Acta Embryol. Morphol. Exp*. **1**, 55–68.
30. Kalová J, Mareš R. 2015 Reference values of surface tension of water. *Int. J. Thermophys*. **36**, 1396–1404. (doi:10.1007/s10765-015-1907-2)
31. Agero U, Glazier JA, Hosek M. 2010 Bulk elastic properties of chicken embryos during somitogenesis. *Biomed. Eng. Online* **9**, 19. (doi:10.1186/1475-925X-9-19)
32. Goldsmith LA, Baden HP. 1971 The mechanical properties of hair II. Chemical modifications and pathological hairs. *J. Invest. Dermatol*. **56**, 200–204. (doi:10.1111/1523-1747.ep12260826)
33. Goriely A, Tabor M. 1998 Spontaneous helix hand reversal and tendril perversion in climbing plants. *Phys. Rev. Lett*. **80**, 1564–1568. (doi:10.1103/PhysRevLett.80.1564)
34. Wang J, Wang G, Feng X-Q, Kitamura T, Kang Y-L, Yu S-W, Qin Q-H. 2013 Hierarchical chirality transfer in the growth of Towel Gourd tendrils. *Sci. Rep*. **3**, 3102. (doi:10.1038/srep03102)
35. Liu J, Huang J, Su T, Bertoldi K, Clarke DR. 2014 Structural transition from helices to hemihelices. *PLoS ONE* **9**, e93183. (doi:10.1371/journal.pone.0093183)
36. Chen Z, Huang G, Trase I, Han X, Mei Y. 2016 Mechanical self-assembly of a strain-engineered flexible layer: Wrinkling, rolling, and twisting. *Phys. Rev. Appl*. **5**, 017001. (doi:10.1103/PhysRevApplied.5.017001)
37. Miller JT, Lazarus A, Audoly B, Reis PM. 2014 Shapes of a suspended curly hair. *Phys. Rev. Lett*. **112**, 068103. (doi:10.1103/PhysRevLett.112.068103)
38. Collignon J, Varlet I, Robertson EJ. 1996 Relationship between asymmetric *nodal* expression and the direction of embryonic turning. *Nature* **381**, 155–158. (doi:10.1038/381155a0)
39. Meno C, Saijoh Y, Fujii H, Ikeda M, Yokoyama T, Yokoyama M, Toyoda Y, Hamada H. 1996 Left–right asymmetric expression of the TGFβ-family member *lefty* in mouse embryos. *Nature* **381**, 151–155. (doi:10.1038/381151a0)
40. Voronov DA, Alford PW, Xu G, Taber LA. 2004 The role of mechanical forces in dextral rotation during cardiac looping in the chick embryo. *Dev. Biol*. **272**, 339–350. (doi:10.1016/j.ydbio.2004.04.033)
41. Ramasubramanian A, Chu-Lagraff QB, Buma T, Chico KT, Carnes ME, Burnett KR, Bradner SA, Gordon SS. 2013 On the role of intrinsic and extrinsic forces in early cardiac S-looping. *Dev. Dyn*. **242**, 801–816. (doi:10.1002/dvdy.23968)
42. Garcia KE, Okamoto RJ, Bayly PV, Taber LA. 2016 Contraction and stress-dependent growth shape the forebrain of the early chicken embryo. *J. Mech. Behav. Biomed. Mater*. **65**, 383–397. (doi:10.1016/j.jmbbm.2016.08.010)
43. Deuchar EM. 1971 The mechanism of axial rotation in the rat embryo: an experimental study *in vitro*. *J. Embryol. Exp. Morphol*. **25**, 189–201.
44. Tee YH *et al.* 2015 Cellular chirality arising from the self-organization of the actin cytoskeleton. *Nat. Cell Biol*. **17**, 445–457. (doi:10.1038/ncb3137)
45. Henley C. 2012 Possible origins of macroscopic left–right asymmetry in organisms. *J. Stat. Phys*. **148**, 741–775. (doi:10.1007/s10955-012-0520-z)
46. Manca A *et al.* 2012 Nerve growth factor regulates axial rotation during early stages of chick embryo development. *Proc. Natl Acad. Sci. USA* **109**, 2009–2014. (doi:10.1073/pnas.1121138109)
47. Poelmann RE, Mentink MM, van Leeuwen JL. 1987 Axial rotation of murine embryos, a study of asymmetric mitotic activity in the neural tube of somite stages. *Anat. Embryol*. (*Berl*) **176**, 99–103. (doi:10.1007/BF00309757)
48. Heyer J, Escalante-Alcalde D, Lia M, Boettinger E, Edelmann W, Stewart CL, Kucherlapati R. 1999 Postgastrulation *Smad2*-deficient embryos show defects in embryo turning and anterior morphogenesis. *Proc. Natl Acad. Sci. USA* **96**, 12 595–12 600. (doi:10.1073/pnas.96.22.12595)
49. Zhu L, Marvin MJ, Gardiner A, Lassar AB, Mercola M, Stern CD, Levin M. 1999 Cerberus regulates left–right asymmetry of the embryonic head and heart. *Curr. Biol*. **9**, 931–938. (doi:10.1016/S0960-9822(99)80419-9)
50. Roebroek AJM, Umans L, Pauli IG, Robertson EJ, van Leuven F, Van de Ven WJ, Constam DB. 1998 Failure of ventral closure and axial rotation in embryos lacking the proprotein convertase Furin. *Development* **125**, 4863–4876.
51. Melloy PG, Ewart JL, Cohen MF, Desmond ME, Kuehn MR, Lo CW. 1998 *No turning*, A mouse mutation causing left–right and axial patterning defects. *Dev. Biol*. **193**, 77–89. (doi:10.1006/dbio.1997.8787)
52. Männer J, Seidl W, Steding G. 1995 Formation of the cervical flexure: an experimental study on chick embryos. *Acta Anat*. **152**, 1–10. (doi:10.1159/000147677)
53. Itasaki N, Nakamura H, Sumida H, Yasuda M. 1991 Actin bundles on the right side in the caudal part of the heart tube play a role in dextro-looping in the embryonic chick heart. *Anat. Embryol*. **183**, 29–39. (doi:10.1007/BF00185832)
54. Lowe LA, Supp DM, Sampath K, Yokoyama T, Wright CVE, Potter SS, Overbeek P, Kuehn MR. 1996 Conserved left–right asymmetry of nodal expression and alterations in murine *situs inversus*. *Nature* **381**, 158–161. (doi:10.1038/381158a0)
55. Esteban CR, Capdevila J, Economides AN, Pascual J, Ortiz Á, Belmonte JCI. 1999 The novel Cer-like protein Caronte mediates the establishment of embryonic left–right asymmetry. *Nature* **401**, 243–251. (doi:10.1038/45738)
56. Levin M. 2009 Perspectives and open problems in the early phases of left–right patterning. *Semin. Cell Dev. Biol*. **20**, 456–463. (doi:10.1016/j.semcdb.2008.11.010)
57. Nonaka S, Shiratori H, Saijoh Y, Hamada H. 2002 Determination of left–right patterning of the mouse embryo by artificial nodal flow. *Nature* **418**, 96–99. (doi:10.1038/nature00849)
58. Güntürkün O. 2003 Human behavior: adult persistence of head-turning asymmetry. *Nature* **421**, 711. (doi:10.1038/421711a)